

# Learning Adaptive Control for $SE(3)$ Hamiltonian Dynamics

Thai Duong

Nikolay Atanasov

**Abstract**—Fast adaptive control is a critical component for reliable robot autonomy in rapidly changing operational conditions. While a robot dynamics model may be obtained from first principles or learned from data, updating its parameters is often too slow for online adaptation to environment changes. This motivates the use of machine learning techniques to learn disturbance descriptors from trajectory data offline as well as the design of adaptive control to estimate and compensate the disturbances online. This paper develops adaptive geometric control for rigid-body systems, such as ground, aerial, and underwater vehicles, that satisfy Hamilton’s equations of motion over the  $SE(3)$  manifold. Our design consists of an offline system identification stage, followed by an online adaptive control stage. In the first stage, we learn a Hamiltonian model of the system dynamics using a neural ordinary differential equation (ODE) network trained from state-control trajectory data with different disturbance realizations. The disturbances are modeled as a linear combination of nonlinear descriptors. In the second stage, we design a trajectory tracking controller with disturbance compensation from an energy-based perspective. An adaptive control law is employed to adjust the disturbance model online proportional to the geometric tracking errors on the  $SE(3)$  manifold. We verify our adaptive geometric controller for trajectory tracking on a fully-actuated pendulum and an under-actuated quadrotor.

## I. INTRODUCTION

Autonomous mobile robots assisting in transportation, search and rescue, and environmental monitoring applications face complex and dynamic operational conditions. Ensuring safe operation in such environments depends on the availability of accurate system dynamics models [1]. This has motivated the development of data-driven approaches, based on Gaussian processes [2]–[7], neural networks [8], [9], and other machine learning techniques [10], to learn dynamics models. Since data-driven dynamics models require large amounts of data, recent works [11]–[15] impose prior knowledge about the system on the model architecture, which a black-box machine learning model might struggle to infer. A physically motivated model structure also simplifies the design of a stable regulation or tracking controller [13]–[15].

Disturbances and system changes during online operation bring about new out-of-distribution data. It is often too slow to re-train the nominal dynamics model to support real-time adaptation to environment changes. Instead, adaptive control [16]–[19] offers efficient tools to estimate and compensate for disturbances and parameter variations online. Recent

work in data-driven adaptive control approximates disturbances as a linear combination of nonlinear features, represented by Gaussian processes [20]–[22] or neural networks [23]–[27]. The disturbance features can be learned online in the control loop [21], [23], [24] or offline from system trajectory data [25]–[28]. The nominal control law is paired with an adaptation law that compensates the disturbances, e.g., using  $\mathcal{L}_1$  adaptation [21] or by updating the last linear layer of the neural network modeling the disturbance features [23]–[27].

This paper develops data-driven adaptive control for rigid-body systems, such as unmanned ground vehicle (UGVs), unmanned aerial vehicle (UAVs), or unmanned underwater vehicles (UUVs), that satisfy Hamilton’s equations of motion over the  $SE(3)$  manifold. Recent techniques for dynamics learning and data-driven adaptive control are mostly restricted to systems whose states evolve in Euclidean space. Our work contributes a dynamics learning approach that respects the system’s kinematic and energy conservation constraints by construction and an adaptive control law that takes geometric tracking error on the  $SE(3)$  manifold into account when attenuating disturbances. Given a dataset of state-control trajectories with different disturbance realizations, we learn a Hamiltonian model of the system dynamics and nonlinear disturbance features using neural ODE networks [15]. In this model, the system potential energy, parameters (mass, inertia, input gain), and external forces (disturbances) are represented by separate neural networks, connected in an architecture that respects the Hamiltonian dynamics structure. We design a tracking controller by shaping the energy of the learned model and pair it with an adaptation law that compensates disturbances online by scaling the learned disturbance features using the  $SE(3)$  tracking error.

In summary, our **contribution** is a learning-based adaptive geometric control approach that

- learns Hamiltonian dynamics on the  $SE(3)$  manifold and a disturbance model offline from state-control trajectories, and
- employs energy-based tracking control with adaptive disturbance compensation online based on the learned models and the geometric tracking errors.

We verify the approach on a fully-actuated pendulum and an under-actuated quadrotor.

## II. RELATED WORK

Adaptive control designs aim to tolerate parametric, structural, or disturbance uncertainties while achieving system stability and asymptotic tracking. A recent comprehensive survey is presented in [29]. Commonly, an adaptation law

We gratefully acknowledge support from NSF RI IIS-2007141 and ARL DCIST CRA W911NF-17-2-0181.

The authors are with the Department of Electrical and Computer Engineering, University of California San Diego, La Jolla, CA 92093, USA, e-mail: {tduong, natanasov}@ucsd.edu.

is an augmentation of an existing nominal controller that adjusts the controller parameters based on performance errors. Self-tuning control (STC) and model reference adaptive control (MRAC) are the two most popular adaptive control methods for linear systems. A key technical issue in nonlinear adaptive control is the parameterization of the system uncertainties [17]. For linearly parameterized systems, disturbances are modeled as linear combinations of known nonlinear features and updated by an adaptation law based on the state errors with stability obtained by, e.g., sliding-mode theory [30]–[35], assuming zero-state detectability [34]–[36] or  $\mathcal{L}_1$ –adaptation [19], [21], [37]. For mechanical systems, such adaptation laws are paired with a nominal controller, derived using Lagrangian dynamics with feedback linearization [30]–[35], Hamiltonian dynamics with energy shaping [34], [35], [38], or model predictive control [37], [39]–[42]. Meanwhile, if the systems evolve on a manifold, e.g.,  $SE(3)$ , an adaptation law is designed based on geometric errors, derived from the manifold constraints [43]–[47].

Recently, there has been growing interest in applying machine learning techniques to design adaptive controllers. Since the nonlinear disturbance features are actually unknown in practice, they can be estimated using Gaussian processes [20]–[22] or neural networks [23]–[27]. The features can be learned from data online in the control loop [21], [23], [24], which is potentially too slow for real-time operation, or offline via meta-learning from past state-control trajectories [25], [26], [28] or simulation of the system dynamics [27]. Given the learned disturbance features, an adaptation law is designed to estimate the disturbances online, e.g. using  $\mathcal{L}_1$  adaptation [21] or by updating the last layer of the feature neural networks [23]–[27], [48]. Besides the disturbance features, the parameters of the adaptive controllers can be learned as well using meta-learning [27].

While prior learning-based adaptive control techniques [23]–[27], [48] rely on Lagrangian dynamics and feedback linearization to design the adaptive trajectory tracking controller, we approach the control design from an energy perspective using Hamiltonian dynamics on the  $SE(3)$  manifold. Compared to adaptive controllers for quadrotors with known  $SE(3)$  dynamics [43]–[47], we develop a general adaptation law based on geometric tracking errors with a disturbance model learned from trajectory data that can be used for any rigid-body robot, such as a UGV, UAV, or UAV.

### III. PROBLEM STATEMENT

Consider a robot modeled as a single rigid body with position  $\mathbf{p} \in \mathbb{R}^3$ , orientation  $\mathbf{R} \in SO(3)$ , body-frame linear velocity  $\mathbf{v} \in \mathbb{R}^3$ , and body-frame angular velocity  $\boldsymbol{\omega} \in \mathbb{R}^3$ . Let  $\mathbf{q} = [\mathbf{p}^\top \mathbf{r}_1^\top \mathbf{r}_2^\top \mathbf{r}_3^\top]^\top \in \mathbb{R}^{12}$  be the generalized coordinates, where  $\mathbf{r}_1, \mathbf{r}_2, \mathbf{r}_3$  are the rows of the rotation matrix  $\mathbf{R}$ . Let  $\boldsymbol{\zeta} = [\mathbf{v}^\top \boldsymbol{\omega}^\top]^\top \in \mathbb{R}^6$  be the generalized velocity. The state  $\mathbf{x} = (\mathbf{q}, \boldsymbol{\zeta})$  evolves on the tangent bundle  $TSE(3)$  of the pose manifold  $SE(3)$  and is governed by the robot dynamics:

$$\dot{\mathbf{x}} = \mathbf{f}(\mathbf{x}, \mathbf{u}, \mathbf{d}), \quad (1)$$

where  $\mathbf{u}$  is the control input and  $\mathbf{d}$  is a disturbance signal. The disturbance  $\mathbf{d}$  is modeled as a linear combination of nonlinear features  $\mathbf{W}(\mathbf{q}, \mathbf{p}) \in \mathbb{R}^{6 \times p}$ :

$$\mathbf{d}(t) = \mathbf{W}(\mathbf{q}(t), \mathbf{p}(t)) \mathbf{a}^*, \quad (2)$$

where  $\mathbf{a}^* \in \mathbb{R}^p$  are unknown feature weights.

As a mechanical system, the robot obeys Hamilton's equations of motion [49]. The generalized momentum of the system is defined as:

$$\mathbf{p} = \mathbf{M}(\mathbf{q}) \boldsymbol{\zeta} \in \mathbb{R}^6, \quad (3)$$

where  $\mathbf{M}(\mathbf{q}) \in \mathbb{R}^{6 \times 6}$  is the generalized mass matrix. The Hamiltonian,  $\mathcal{H}(\mathbf{q}, \mathbf{p})$ , captures the total energy of the system as the sum of the kinetic energy  $T(\mathbf{q}, \mathbf{p}) = \frac{1}{2} \mathbf{p}^\top \mathbf{M}(\mathbf{q})^{-1} \mathbf{p}$  and the potential energy  $V(\mathbf{q})$ :

$$\mathcal{H}(\mathbf{q}, \mathbf{p}) = \frac{1}{2} \mathbf{p}^\top \mathbf{M}(\mathbf{q})^{-1} \mathbf{p} + V(\mathbf{q}). \quad (4)$$

The system dynamics are governed by the Hamiltonian:

$$\begin{bmatrix} \dot{\mathbf{q}} \\ \dot{\mathbf{p}} \end{bmatrix} = \begin{bmatrix} \mathbf{0} & \mathbf{q}^\times \\ -\mathbf{q}^{\times\top} & \mathbf{p}^\times \end{bmatrix} \begin{bmatrix} \frac{\partial \mathcal{H}}{\partial \mathbf{q}} \\ \frac{\partial \mathcal{H}}{\partial \mathbf{p}} \end{bmatrix} + \begin{bmatrix} \mathbf{0} \\ \mathbf{g}(\mathbf{q}) \end{bmatrix} \mathbf{u} + \begin{bmatrix} \mathbf{0} \\ \mathbf{d} \end{bmatrix}, \quad (5)$$

where the disturbance  $\mathbf{d}$  appears as an external force applied to the system. The system parameters are the input gain  $\mathbf{g}(\mathbf{q})$ , mass  $\mathbf{M}(\mathbf{q})$ , potential energy  $V(\mathbf{q})$ , disturbance features  $\mathbf{W}(\mathbf{q}, \mathbf{p})$ , and disturbance feature weights  $\mathbf{a}$ . The cross maps  $\mathbf{q}^\times$  and  $\mathbf{p}^\times$  are defined as:

$$\mathbf{q}^\times = \begin{bmatrix} \mathbf{R}^\top & \mathbf{0} & \mathbf{0} & \mathbf{0} \\ \mathbf{0} & \hat{\mathbf{r}}_1^\top & \hat{\mathbf{r}}_2^\top & \hat{\mathbf{r}}_3^\top \end{bmatrix}^\top, \quad \mathbf{p}^\times = \begin{bmatrix} \mathbf{p}_v \\ \mathbf{p}_\omega \end{bmatrix}^\times = \begin{bmatrix} \mathbf{0} & \hat{\mathbf{p}}_v \\ \hat{\mathbf{p}}_v & \hat{\mathbf{p}}_\omega \end{bmatrix},$$

where the hat map  $(\hat{\cdot}) : \mathbb{R}^3 \mapsto \mathfrak{so}(3)$  constructs a skew-symmetric matrix from a 3D vector. From (3), the time derivative of the generalized velocity is:

$$\dot{\boldsymbol{\zeta}} = \left( \frac{d}{dt} \mathbf{M}^{-1}(\mathbf{q}) \right) \mathbf{p} + \mathbf{M}^{-1}(\mathbf{q}) \dot{\mathbf{p}}. \quad (6)$$

In summary, (5) and (6) capture the structure of the system dynamics  $\dot{\mathbf{x}} = \mathbf{f}(\mathbf{x}, \mathbf{u}, \mathbf{d})$ .

Consider a collection  $\mathcal{D} = \{\mathcal{D}_1, \mathcal{D}_2, \dots, \mathcal{D}_M\}$  of state-control trajectory datasets  $\mathcal{D}_j$ , each collected under a different unknown disturbance realization  $\mathbf{a}_j^*$ , for  $j = 1, \dots, M$ . A trajectory dataset  $\mathcal{D}_j = \{t_{0:N}^{(ij)}, \mathbf{x}_{0:N}^{(ij)}, \mathbf{u}^{(ij)}\}_{i=1}^{D_j}$  consists of  $D_j$  state sequences  $\mathbf{x}_{0:N}^{(ij)}$ , obtained by applying a constant control input  $\mathbf{u}^{(ij)}$  to the system with initial condition  $\mathbf{x}_0^{(ij)}$  at time  $t_0^{(ij)}$  and sampling its state  $\mathbf{x}^{(ij)}(t_n^{(ij)}) =: \mathbf{x}_n^{(ij)}$  at times  $t_0^{(ij)} < t_1^{(ij)} < \dots < t_N^{(ij)}$ . Our objective is to approximate the dynamics  $\mathbf{f}$  by  $\mathbf{f}_\theta$ , where the parameters  $\theta$  characterize the unknowns  $\mathbf{M}_\theta(\mathbf{q})$ ,  $V_\theta(\mathbf{q})$ ,  $\mathbf{g}_\theta(\mathbf{q})$ , as well as the disturbance model in (2) by  $\mathbf{W}_\phi(\mathbf{q}, \mathbf{p}) \mathbf{a}_j$ , where the parameters  $\phi$ ,  $\{\mathbf{a}_j\}_{j=1}^M$  model each disturbance sample. To optimize  $\theta$ ,  $\phi$ ,  $\{\mathbf{a}_j\}$ , we roll out the approximated dynamics starting from state  $\mathbf{x}_0^{(ij)}$  with a constant control  $\mathbf{u}^{(ij)}$  and minimize the distance between the predicted state sequence  $\bar{\mathbf{x}}_{1:N}^{(ij)}$  and the true state sequence  $\mathbf{x}_{1:N}^{(ij)}$  from  $\mathcal{D}_j$ , for  $j = 1, \dots, M$ .

**Problem 1.** Given  $\mathcal{D} = \{\{t_{0:N}^{(ij)}, \mathbf{x}_{0:N}^{(ij)}, \mathbf{u}^{(ij)}\}_{i=1}^{D_j}\}_{j=1}^M$ , find parameters  $\theta, \phi, \{\mathbf{a}_j\}_{j=1}^M$  that minimize:

$$\begin{aligned} \min_{\theta, \phi, \{\mathbf{a}_j\}} & \sum_{j=1}^M \sum_{i=1}^{D_j} \sum_{n=1}^N \ell(\mathbf{x}_n^{(ij)}, \bar{\mathbf{x}}_n^{(ij)}) \\ \text{s.t. } & \dot{\bar{\mathbf{x}}}^{(ij)}(t) = \bar{\mathbf{f}}_\theta(\bar{\mathbf{x}}^{(ij)}(t), \mathbf{u}^{(ij)}, \bar{\mathbf{d}}^{(ij)}(t)), \\ & \bar{\mathbf{d}}^{(ij)}(t) = \mathbf{W}_\phi(\bar{\mathbf{x}}^{(ij)}(t))\mathbf{a}_j, \\ & \bar{\mathbf{x}}^{(ij)}(t_0) = \mathbf{x}_0^{(ij)}, \quad \bar{\mathbf{x}}_n^{(ij)} = \bar{\mathbf{x}}^{(ij)}(t_n), \\ & \forall j = 1, \dots, M, \quad \forall n = 1, \dots, N, \quad \forall i = 1, \dots, D_j, \end{aligned} \quad (7)$$

where  $\ell$  is a distance metric on the state space  $TSE(3)$ .

After the offline system identification in Problem 1, we aim to design a controller  $\mathbf{u} = \pi(\mathbf{x}, \mathbf{x}^*, \mathbf{a}; \theta, \phi)$  that tracks a desired state trajectory  $\mathbf{x}^*(t)$ ,  $t \geq t_0$ , using the learned dynamics  $\bar{\mathbf{f}}_\theta$  and disturbance  $\mathbf{W}_\phi$  models. To handle disturbance realizations  $\mathbf{d} = \mathbf{W}_\phi(\mathbf{x})\mathbf{a}^*$  with unknown ground-truth  $\mathbf{a}^*$ , we augment the tracking controller with an adaptation law  $\dot{\mathbf{a}} = \rho(\mathbf{x}, \mathbf{x}^*, \mathbf{a}; \phi)$  that estimates  $\mathbf{a}^*$  online.

**Problem 2.** Given an initial condition  $\mathbf{x}_0$  at time  $t_0$ , desired state trajectory  $\mathbf{x}^*(t)$ ,  $t \geq t_0$ , learned dynamics  $\bar{\mathbf{f}}_\theta$  and learned disturbance features  $\mathbf{W}_\theta$ , design an adaptive controller, coupling a tracking law  $\mathbf{u} = \pi(\mathbf{x}, \mathbf{x}^*, \mathbf{a}; \theta, \phi)$  and an adaptation law  $\dot{\mathbf{a}} = \rho(\mathbf{x}, \mathbf{x}^*, \mathbf{a}; \phi)$  such that  $\limsup_{t \rightarrow \infty} \ell(\mathbf{x}(t), \mathbf{x}^*(t))$  is bounded.

#### IV. TECHNICAL APPROACH

We present our approach in two stages: Hamiltonian-based dynamics learning to solve Problem 1 (Sec. IV-A) and adaptive control design to solve Problem 2 (Sec. IV-B).

##### A. Hamiltonian-based dynamics learning with disturbances

To address Problem 1, we use a neural ODE network [50] whose structure respects Hamilton's equations in (5) and, hence, guarantees satisfaction of the  $SE(3)$  kinematic constraints and energy conservation by construction. We extend our prior work on Hamiltonian neural ODE learning [15] by introducing a disturbance model,  $\mathbf{d} = \mathbf{W}_\phi(\mathbf{q}, \mathbf{p})\mathbf{a}$ , and estimating its parameters  $\phi, \mathbf{a}$  along with the system dynamics parameters  $\theta$ .

Each training set  $\mathcal{D}_j = \{\{t_{0:N}^{(ij)}, \mathbf{x}_{0:N}^{(ij)}, \mathbf{u}^{(ij)}\}_i\}$  is generated by applying a constant input  $\mathbf{u}^{(ij)}$  to the system and sampling the state  $\mathbf{x}_n^{(ij)} = \mathbf{x}^{(n)}(t_n^{(ij)})$  at times  $t_n^{(ij)}$  for  $n = 0, \dots, N$  using an odometry algorithm [51], [52] or a motion capture system. The data collection can be performed using an existing baseline controller or a human operator manually controlling the robot under different disturbance conditions (e.g., wind, ground effect, etc. for a UAV).

We define the  $TSE(3)$  distance metric  $\ell$  in Problem 1 as a sum of position, orientation, and velocity errors:

$$\ell(\mathbf{x}, \bar{\mathbf{x}}) = \ell_{\mathbf{p}}(\mathbf{x}, \bar{\mathbf{x}}) + \ell_{\mathbf{R}}(\mathbf{x}, \bar{\mathbf{x}}) + \ell_{\dot{\mathbf{x}}}(\mathbf{x}, \bar{\mathbf{x}}), \quad (8)$$

defined as follows:

$$\begin{aligned} \ell_{\mathbf{p}}(\mathbf{x}, \bar{\mathbf{x}}) &= \|\mathbf{p} - \bar{\mathbf{p}}\|_2^2, & \ell_{\dot{\mathbf{x}}}(\mathbf{x}, \bar{\mathbf{x}}) &= \|\dot{\mathbf{x}} - \bar{\dot{\mathbf{x}}}\|_2^2, \\ \ell_{\mathbf{R}}(\mathbf{x}, \bar{\mathbf{x}}) &= \|(\log(\bar{\mathbf{R}}\mathbf{R}^\top))^\vee\|_2^2, \end{aligned}$$

where  $\log : SE(3) \mapsto \mathfrak{se}(3)$  is the inverse of the exponential map, associating a rotation matrix to a skew-symmetric matrix, and  $(\cdot)^\vee : \mathfrak{se}(3) \mapsto \mathbb{R}^3$  is the inverse of the hat map  $(\cdot)$ . Let  $\mathcal{L}(\theta, \phi, \{\mathbf{a}_j\}; \mathcal{D})$  be the total loss in Problem 1. To calculate the loss, for each dataset  $\mathcal{D}_j$  with disturbance  $\bar{\mathbf{d}}^{(ij)}(t) = \mathbf{W}_\phi(\bar{\mathbf{x}}^{(ij)}(t))\mathbf{a}_j$ , we solve an ODE:

$$\dot{\bar{\mathbf{x}}}^{(ij)} = \bar{\mathbf{f}}_\theta(\bar{\mathbf{x}}^{(ij)}, \mathbf{u}^{(ij)}, \bar{\mathbf{d}}^{(ij)}), \quad \bar{\mathbf{x}}^{(ij)}(0) = \mathbf{x}_0^{(ij)}, \quad (9)$$

using an ODE solver [50]. This generates a predicted system state trajectory  $\bar{\mathbf{x}}_{1:N}^{(ij)}$  at times  $t_{1:N}^{(ij)}$  for each  $i = 1, \dots, D_j$  and  $j = 1, \dots, M$ , sufficient to compute  $\mathcal{L}(\theta, \phi, \{\mathbf{a}_j\}; \mathcal{D})$ . The parameters  $\theta, \phi$ , and  $\mathbf{a}_j$  are updated using gradient descent by back-propagating the loss through the neural ODE solver using adjoint states. See [50] and [15] for details.

##### B. Data-driven geometric adaptive control

We address Problem 2 by developing a trajectory tracking controller  $\pi$  that compensates for disturbance and an adaptation law  $\rho$  that estimates the disturbances online.

We develop a tracking controller  $\pi$  for the learned Hamiltonian dynamics using the interconnection and damping assignment passivity-based control (IDA-PBC) method [53]. Consider a desired state trajectory  $\mathbf{x}^*(t) = (\mathbf{q}^*(t), \dot{\mathbf{q}}^*(t))$ . Since the momentum  $\mathbf{p}$  in (3) is defined in the body inertial frame, the desired momentum  $\mathbf{p}^*(t)$  should be computed by transforming the desired velocity  $\dot{\mathbf{q}}^* = [\mathbf{v}^{*\top} \quad \boldsymbol{\omega}^{*\top}]^\top$  to the body frame as  $\mathbf{p}^* = \mathbf{M}(\mathbf{q}) \begin{bmatrix} \mathbf{R}^\top \mathbf{R}^* \mathbf{v}^* \\ \mathbf{R}^\top \mathbf{R}^* \boldsymbol{\omega}^* \end{bmatrix}$ . The Hamiltonian of the system in (4) is not necessarily minimized along  $(\mathbf{q}^*(t), \mathbf{p}^*(t))$ . The key idea of the IDA-PBC design is to choose the control input  $\mathbf{u}(t)$  so that the closed-loop system has a desired Hamiltonian  $\mathcal{H}_d(\mathbf{q}, \mathbf{p})$ , which is minimized along  $(\mathbf{q}^*(t), \mathbf{p}^*(t))$ . Using a quadratic error on the tangent bundle  $TSE(3)$ , we design the desired Hamiltonian:

$$\begin{aligned} \mathcal{H}_d(\mathbf{q}, \mathbf{p}) &= \frac{1}{2} k_{\mathbf{p}} (\mathbf{p} - \mathbf{p}^*)^\top (\mathbf{p} - \mathbf{p}^*) \\ &+ \frac{1}{2} k_{\mathbf{R}} \text{tr}(\mathbf{I} - \mathbf{R}^* \mathbf{R}) + \frac{1}{2} (\mathbf{p} - \mathbf{p}^*)^\top \mathbf{M}^{-1}(\mathbf{q}) (\mathbf{p} - \mathbf{p}^*), \end{aligned} \quad (10)$$

where  $k_{\mathbf{p}}$  and  $k_{\mathbf{R}}$  are positive gains. We solve a set of matching conditions, described in [15], [53], between the original dynamics with Hamiltonian  $\mathcal{H}$  in (4) and the desired dynamics with Hamiltonian  $\mathcal{H}_d$  in (10) to arrive at a tracking controller  $\mathbf{u} = \pi(\mathbf{x}, \mathbf{x}^*, \mathbf{a}; \theta, \phi)$ . The controller consists of an energy-shaping term  $\mathbf{u}_{ES}$ , a damping-injection term  $\mathbf{u}_{DI}$ , and a disturbance compensation term  $\mathbf{u}_{DC}$ :

$$\begin{aligned} \mathbf{u}_{ES} &= \mathbf{g}^\dagger(\mathbf{q}) \left( \mathbf{q}^{\times\top} \frac{\partial V}{\partial \mathbf{q}} - \mathbf{p}^\times \mathbf{M}^{-1}(\mathbf{q}) \mathbf{p} - \mathbf{e}(\mathbf{q}, \mathbf{q}^*) + \dot{\mathbf{p}}^* \right), \\ \mathbf{u}_{DI} &= -\mathbf{K}_d \mathbf{g}^\dagger(\mathbf{q}) \mathbf{M}^{-1}(\mathbf{q}) (\mathbf{p} - \mathbf{p}^*), \\ \mathbf{u}_{DC} &= -\mathbf{g}^\dagger(\mathbf{q}) \mathbf{W}(\mathbf{q}, \mathbf{p}) \mathbf{a}, \end{aligned} \quad (11)$$

where  $\mathbf{g}^\dagger(\mathbf{q}) = (\mathbf{g}^\top(\mathbf{q})\mathbf{g}(\mathbf{q}))^{-1} \mathbf{g}^\top(\mathbf{q})$  is the pseudo-inverse of  $\mathbf{g}(\mathbf{q})$  and  $\mathbf{K}_d = \text{diag}(k_{\mathbf{v}}\mathbf{I}, k_{\boldsymbol{\omega}}\mathbf{I})$  is a damping gain with positive terms  $k_{\mathbf{v}}, k_{\boldsymbol{\omega}}$ . The controller utilizes a generalized coordinate error between  $\mathbf{q}$  and  $\mathbf{q}^*$ :

$$\mathbf{e}(\mathbf{q}, \mathbf{q}^*) = \begin{bmatrix} \mathbf{e}_{\mathbf{p}}(\mathbf{q}, \mathbf{q}^*) \\ \mathbf{e}_{\mathbf{R}}(\mathbf{q}, \mathbf{q}^*) \end{bmatrix} = \begin{bmatrix} k_{\mathbf{p}} \mathbf{R}^\top (\mathbf{p} - \mathbf{p}^*) \\ \frac{1}{2} k_{\mathbf{R}} (\mathbf{R}^* \mathbf{R} - \mathbf{R}^\top \mathbf{R}^*)^\vee \end{bmatrix} \quad (12)$$

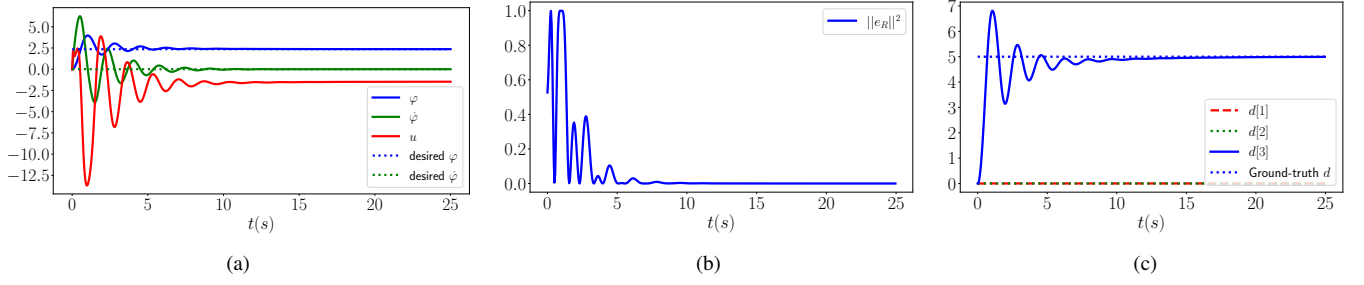


Fig. 1: Evaluation of our learned adaptive controller on a pendulum: (a) the angle  $\varphi$ , its velocity  $\dot{\varphi}$  are driven to their desired values; (b) the geometric error  $\|\mathbf{e}_R\|^2$  converges to 0 and (c) The disturbance estimated by our adaptation law  $\boldsymbol{\rho}$  converges to the ground-truth value.

and a generalized momentum error between  $\mathbf{p}$  and  $\mathbf{p}^*$ :

$$\mathbf{p} - \mathbf{p}^* = \mathbf{M}(\mathbf{q}) \begin{bmatrix} \mathbf{e}_v(\mathbf{x}, \mathbf{x}^*) \\ \mathbf{e}_\omega(\mathbf{x}, \mathbf{x}^*) \end{bmatrix} = \mathbf{M}(\mathbf{q}) \begin{bmatrix} \mathbf{v} - \mathbf{R}^\top \mathbf{R}^* \mathbf{v}^* \\ \boldsymbol{\omega} - \mathbf{R}^\top \mathbf{R}^* \boldsymbol{\omega}^* \end{bmatrix}. \quad (13)$$

Please refer to [15] for a detailed derivation of  $\mathbf{u}_{ES}$  and  $\mathbf{u}_{DI}$ .

Our prior work did not include the disturbance compensation term  $\mathbf{u}_{DC}$  in (11), which requires online estimation of the disturbance feature weights  $\mathbf{a}$ . Inspired by [31], we design an adaptation law which utilizes the body-frame geometric errors in (12), (13) to update the disturbance feature weights:

$$\begin{aligned} \dot{\mathbf{a}} &= \boldsymbol{\rho}(\mathbf{x}, \mathbf{x}^*, \mathbf{a}; \phi) \\ &= \mathbf{W}_\phi^\top(\mathbf{q}, \mathbf{p}) \begin{bmatrix} c_p \mathbf{e}_p(\mathbf{q}, \mathbf{q}^*) + c_v \mathbf{e}_v(\mathbf{x}, \mathbf{x}^*) \\ c_R \mathbf{e}_R(\mathbf{q}, \mathbf{q}^*) + c_\omega \mathbf{e}_\omega(\mathbf{x}, \mathbf{x}^*) \end{bmatrix}, \end{aligned} \quad (14)$$

where  $c_p, c_v, c_R, c_\omega$  are positive coefficients. The stability of our geometric adaptive controller  $(\boldsymbol{\pi}, \boldsymbol{\rho})$  is shown in Theorem 1, with a brief proof in Sec. VII, inspired by [45].

**Theorem 1.** *Consider the Hamiltonian dynamics in (5) with disturbance model in (2). Suppose that the parameters  $\mathbf{g}(\mathbf{q})$ ,  $\mathbf{M}(\mathbf{q})$ ,  $V(\mathbf{q})$ , and  $\mathbf{W}(\mathbf{q}, \mathbf{p})$  are known but the disturbance feature weights  $\mathbf{a}^*$  are unknown. Let  $\mathbf{x}^*(t)$ ,  $t \geq t_0$  be a desired state trajectory with bounded angular velocity,  $\|\boldsymbol{\omega}^*(t)\| \leq \gamma$ . Assume that the initial system state satisfies:*

$$\text{tr}(\mathbf{I} - \mathbf{R}^{*\top}(t_0)\mathbf{R}(t_0)) < \alpha < 2, \quad \|\mathbf{e}_\omega(\mathbf{x}(t_0), \mathbf{x}^*(t_0))\| \leq \beta \quad (15)$$

*for some constants  $\alpha, \beta$ . Consider the tracking controller in (11) with adaptation law in (14). Then, there exist positive constants  $k_p, k_R, k_v, k_\omega, c_p, c_R, c_v, c_\omega$  such that the tracking errors  $\mathbf{e}(\mathbf{q}, \mathbf{q}^*)$  and  $\mathbf{p}_e = \mathbf{p} - \mathbf{p}^*$  defined in (12) and (13) converge to zero. Also, the estimation error  $\mathbf{e}_a = \mathbf{a} - \mathbf{a}^*$  is stable in the sense of Lyapunov and uniformly bounded.*

## V. EVALUATION

We verify the effectiveness of our adaptive controller using a fully-actuated pendulum and an under-actuated quadrotor.

### A. Pendulum

We consider a pendulum with angle  $\varphi$  with respect to the vertically downward position and a scalar control input  $u$ . Assuming that the control input is offset by an unknown disturbance  $d$ , the ground-truth dynamics of the pendulum is  $\ddot{\varphi} = -15 \sin \varphi + 3(u + d)$ , where the ground-truth

mass, potential energy, and the input coefficient are:  $m = 1/3$ ,  $V(\varphi) = 5(1 - \cos \varphi)$ , and  $g(\varphi) = 1$ , respectively.

We modify an OpenAI Gym environment, provided by [14] with the pendulum dynamics, to include the disturbance  $d$  and collect data of the form  $\{(\cos \varphi, \sin \varphi, \dot{\varphi})\}$ . To illustrate our manifold-constrained adaptive control learning, we consider  $\varphi$  as a yaw angle, i.e the rotation matrix  $\mathbf{R}$  describes a rotation around the  $z$  axis. As a result, we use angular velocity of the form:  $\boldsymbol{\omega} = [0, 0, \dot{\varphi}]$ . We remove position  $\mathbf{p}$  and linear velocity  $\mathbf{v}$  from the Hamilton's equations (5), i.e. the state lies on the  $SO(3)$  manifold with generalized coordinates  $\mathbf{q} = [\mathbf{r}_1^\top \quad \mathbf{r}_2^\top \quad \mathbf{r}_3^\top]^\top \in \mathbb{R}^9$ .

In the offline dynamics learning stage (Sec. IV-A), we consider  $M = 11$  samples of the disturbance  $d_j = 0.4(j - 6) \in [-2, 2]$  for  $j = 1, \dots, M$ . For each value  $d_j$ , we collect a dataset  $\mathcal{D}_j = \left\{ (t_{0:N}^{(ij)}, \mathbf{q}_{0:N}^{(ij)}, \boldsymbol{\omega}_{0:N}^{(ij)}, u^{(ij)}) \right\}_{i=1}^{D_j}$  with  $N = 1, D_j = 950$  by applying 950 random control inputs to the pendulum for a time interval of 0.05s. We train the approximated dynamics  $\tilde{\mathbf{f}}$  with disturbance as described in Sec. IV-A for 5000 iterations with learning rate  $10^{-4}$ .

We verify our adaptive controller  $(\boldsymbol{\pi}, \boldsymbol{\rho})$  in Sec. IV-B with a constant desired angle  $\mathbf{x}^* = \varphi^*$  and zero desired velocity  $\dot{\varphi}^* = 0$ . We simplify the energy-based controller  $\boldsymbol{\pi}$  in (11) and the adaptation law  $\boldsymbol{\rho}$  in (14) by removing the position components. The controller gains are chosen as follows:  $k_R = 0.5$ ,  $k_d = 0.1$ ,  $c_R = 1.0$ ,  $c_\omega = 0.5$ . We set the disturbance  $d = 5$ , outside of its sampling range  $[-2, 2]$  for training, and choose the desired angle as  $\varphi^* = 3\pi/4$ . Fig. 1a and 1b shows that we achieved the desired pendulum angle  $\varphi$ , angular velocity  $\dot{\varphi}$  while the control  $u$  converges to a non-zero constant, balancing out the disturbance. Fig. 1c shows that the estimated disturbance  $\mathbf{d} \in \mathbb{R}^3$  converges to the ground truth value  $\mathbf{d} = [0 \quad 0 \quad 5]^\top$ .

### B. Crazyflie Quadrotor

Next, we consider a Crazyflie quadrotor, simulated using the PyBullet physics engine [54], with control input  $\mathbf{u} = [f, \boldsymbol{\tau}]$  including a thrust  $f \in \mathbb{R}_{\geq 0}$  and a torque vector  $\boldsymbol{\tau} \in \mathbb{R}^3$  generated by the 4 rotors. The disturbance  $\mathbf{d}$  comes from two sources: 1) horizontal winds, simulated as an external force  $\mathbf{d}_w = [d_{wx} \quad d_{wy} \quad 0]^\top \in \mathbb{R}^3$  in the world frame, i.e.  $\mathbf{R}^\top \mathbf{d}_w$  in the body frame, applied on the quadrotor, and 2) two defective rotors 1 and 2, generating  $\delta_1$  and  $\delta_2$  percents of the nominal thrust, respectively.

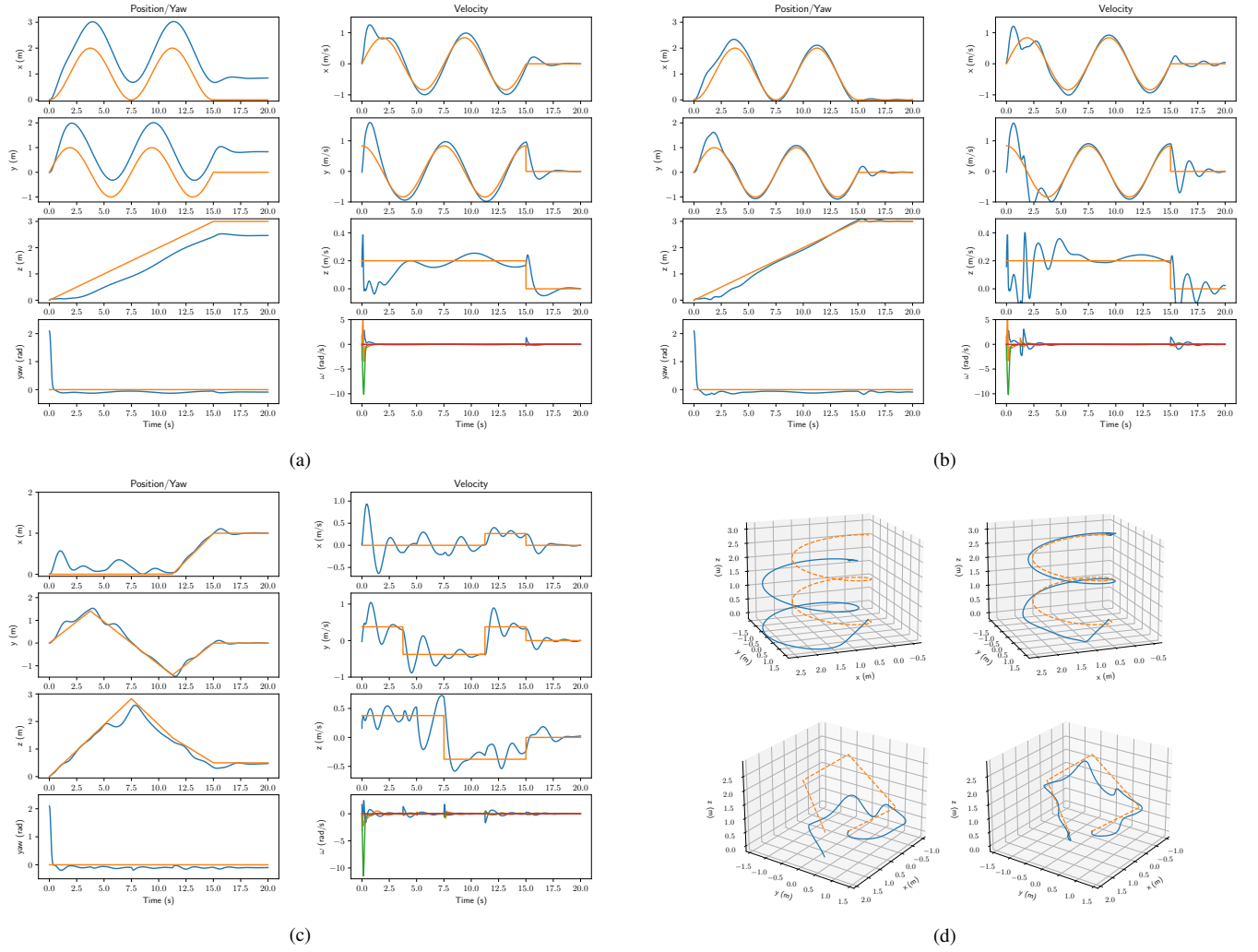


Fig. 2: Tracking spiral and diamond-shaped trajectories with a PyBullet Crazyflie quadrotor [54] in two scenarios: 1) constant wind and defective rotors; and 2) constant wind and good rotors turning defective after 5s: (a) scenario 1 without adaptation, (b) scenario 1 with adaptation, (c) scenario 2 with adaptation. Fig. 2d visualizes tracking results for scenarios 1 (top) and 2 (bottom) with and without adaptation (right and left, respectively). In scenario 2, the quadrotor without adaptation crashes to the ground after 12.5s as seen in Fig. 2d (bottom-left). With adaptation, our controller is able to estimate and compensate for the disturbances and track the trajectory successfully.

We collect a dataset  $\mathcal{D} = \{\mathcal{D}_j\}_{j=1}^M$  with  $M = 8$  realizations of the disturbance  $\mathbf{d}_{wj}$ ,  $\delta_{1j}$  and  $\delta_{2j}$ . Specifically, the wind components  $w_{xj}, w_{yj}$  are chosen from the set  $\{\pm 0.25, \pm 0.5\}$  while the values of  $\delta_{1j}$  and  $\delta_{2j}$  are sampled from the range  $[94\%, 98\%]$ . For each disturbance realization, a PID controller provided by [54] is used to drive the quadrotor from a random starting point to 9 different desired poses. The collected trajectories provides a dataset  $\mathcal{D}_j = \{\mathbf{x}_{0:N}^{(ij)}, \mathbf{q}_{0:N}^{(ij)}, \boldsymbol{\zeta}_{0:N}^{(ij)}, \mathbf{u}^{(ij)}\}_{i=1}^{D_j}$  with  $N = 5$  and  $D_j = 1080$ .

Since the mass  $m$  of the quadrotor is easily measured, we use the ground-truth value  $m = 0.027\text{kg}$  and form our approximated generalized mass matrix as  $\mathbf{M}_\theta(\mathbf{q}) = \text{diag}(m\mathbf{I}, \mathbf{J}_\theta(\mathbf{q}))$ , where  $\mathbf{J}_\theta(\mathbf{q})$  represents an unknown inertial matrix, learned from data. The known mass  $m$  leads to a known potential energy  $V(\mathbf{q}) = mg \begin{bmatrix} 0 & 0 & 1 \end{bmatrix} \mathbf{p}$ , where  $\mathbf{p}$  is the position of the quadrotor and  $g \approx 9.8\text{ms}^{-2}$  is the gravitational acceleration. As described in Sec. IV-A, we learn  $\mathbf{M}_\theta(\mathbf{q})$ ,  $\mathbf{g}_\theta(\mathbf{q})$  and  $\mathbf{W}_\phi(\mathbf{q}, \mathbf{p})$  from the dataset  $\mathcal{D}$ .

We verify our learned adaptive controller in Sec. IV-B by driving the quadrotor to track a pre-defined trajectory in the present of the aforementioned disturbance  $\mathbf{d}$ . The desired trajectory is specified by the desired position  $\mathbf{p}^*(t)$  and the desired heading  $\psi^*(t)$ . We construct an appropriate choice of  $\mathbf{R}^* = [\mathbf{r}_1^* \ \mathbf{r}_2^* \ \mathbf{r}_3^*]$  and  $\boldsymbol{\omega}^*$  to be used with the adaptive controller, similar to [15], [45], [55]. Specifically, the trajectory tracking controller in (11) is re-written as:

$$\mathbf{u} = \mathbf{g}^\dagger(\mathbf{q}) \begin{bmatrix} \mathbf{u}_v \\ \mathbf{u}_\omega \end{bmatrix} = \mathbf{g}^\dagger(\mathbf{q}) \left( \begin{bmatrix} \mathbf{b}_v \\ \mathbf{b}_\omega \end{bmatrix} - \mathbf{W}_\phi(\mathbf{q}, \mathbf{p}) \mathbf{a} \right), \quad (16)$$

where  $\mathbf{b}_v, \mathbf{b}_\omega$  is derived from  $\mathbf{u}_{ES}$  and  $\mathbf{u}_{DI}$  in (11), with gains  $k_p = 0.135$ ,  $k_v = 0.0675$ ,  $k_R = 1.0$ , and  $k_\omega = 0.08$ .

To calculate  $\mathbf{R}^*$  and  $\boldsymbol{\omega}^*$ , the normalized desired thrust in the world frame  $\mathbf{R}\mathbf{u}_v$  should be the  $z$  axis of the body frame, i.e. the third column  $\mathbf{r}_3^*$ . The second column  $\mathbf{r}_2^*$  is constructed so that  $\mathbf{R}^*$  has the desired yaw angle  $\psi^*$ , by projecting  $\mathbf{r}^\psi = [-\sin \psi, \cos \psi, 0]$  onto the plane perpendicular to  $\mathbf{r}_3^*$ . The



first column and the desired angular velocity are:  $\mathbf{r}_1^* = \mathbf{r}_2^* \times \mathbf{r}_3^*$  and  $\boldsymbol{\omega}^* = (\mathbf{R}^{*\top} \dot{\mathbf{R}}^*)^\vee$ , respectively.

Plugging  $\mathbf{R}^*$  and  $\boldsymbol{\omega}^*$  back in (16), we obtain the complete control input  $\mathbf{u}$  that compensates for the disturbances. The disturbances  $\mathbf{d}$  is estimated by updating the weights  $\mathbf{a}$  according to the adaptation law (14) with gains  $c_p = 0.04, c_v = 0.04, c_R = 0.5$ , and  $c_\omega = 0.5$ .

We test the learned adaptive controller in 2 scenarios: 1) tracking a spiral trajectory with a constant wind  $\mathbf{d}_w = [0.75 \ 0.75 \ 0]^\top$ , and defective rotors 1&2 with  $(\delta_1, \delta_2) = (0.8, 0.8)$ ; and 2) tracking a diamond-shaped trajectory with constant winds  $\mathbf{d}_w = [0.8 \ 0.8 \ 0]^\top$ , and rotors 1&2 becoming defective starting at  $t = 5s$  with  $\delta_1 = \delta_2 = 75\%$ . These disturbance realizations lie outside of the disturbance ranges used for training. The near-ground, drag and down-wash effects are also enabled in the PyBullet simulated quadrotor during testing. In scenario 1, the quadrotor without adaptation drifts as seen in Fig. 2a and 2d (upper-left). Meanwhile, Fig. 2b and 2d (upper-right) show that our adaptive controller is able to estimate the disturbance online after a few seconds and successfully tracks the trajectory. In scenario 2, the quadrotor with our controller starts to track the trajectory, then drops down at time  $t = 5s$ , due to the defective rotors, but recovers as our adaptation law updates the disturbance accordingly, as seen in Fig. 2c and 2d (lower-right). Without adaptation, the quadrotor crashes to the ground at  $t \approx 12.5s$ , plotted in Fig. 2d (lower-left).

## VI. CONCLUSION

This paper introduced a gray-box model for rigid-body dynamics learning from disturbance-corrupted trajectory data. We developed a Hamiltonian neural ODE architecture which captures external force disturbances and respects the  $SE(3)$  kinematic constraints and energy conservation of the system by construction. To enable trajectory tracking with on-line disturbance compensation, we design a passivity-based tracking controller and augment it with an adaptation law that compensates disturbances relying on geometric tracking errors. Our evaluation shows that our geometric adaptive controller is able to quickly estimate the disturbance online and successfully tracks the desired trajectory. Future work will focus on evaluating the controller on a real robot system.

## VII. PROOF OF THM. 1

The stability analysis is developed in the domain  $\mathcal{T} = \{\mathbf{x} \in TSE(3) \mid \text{tr}(\mathbf{I} - \mathbf{R}^{*\top} \mathbf{R}) < \alpha < 2, \|\mathbf{e}_\omega(\mathbf{x}, \mathbf{x}^*)\| < \beta\}$ . Since  $\text{tr}(\mathbf{I} - \mathbf{R}^{*\top} \mathbf{R}) < \alpha < 2$ , then  $\|\mathbf{e}_R\|_2^2 \leq \text{tr}(\mathbf{I} - \mathbf{R}^{*\top} \mathbf{R}) \leq \frac{2-\alpha}{2} \|\mathbf{e}_R\|_2^2$  by [56, Prop. 1]. We drop function parameters to simplify the notation. The derivative of the generalized coordinate error satisfies:

$$\begin{aligned} \dot{\mathbf{e}} &= \begin{bmatrix} \dot{\mathbf{e}}_p \\ \dot{\mathbf{e}}_R \end{bmatrix} = \begin{bmatrix} -\hat{\boldsymbol{\omega}} \mathbf{e}_p + k_p \mathbf{e}_v \\ k_R \mathbf{E}(\mathbf{R}, \mathbf{R}^*) \mathbf{e}_\omega \end{bmatrix}, \\ &= - \begin{bmatrix} \hat{\boldsymbol{\omega}} & \mathbf{0} \\ \mathbf{0} & \mathbf{0} \end{bmatrix} \mathbf{e} + \begin{bmatrix} k_p \mathbf{I} & \mathbf{0} \\ \mathbf{0} & k_R \mathbf{E}(\mathbf{R}, \mathbf{R}^*) \end{bmatrix} \mathbf{M}^{-1} \mathbf{p}_e, \end{aligned} \quad (17)$$

where  $\mathbf{E}(\mathbf{R}, \mathbf{R}^*) = \frac{1}{2}(\text{tr}(\mathbf{R}^\top \mathbf{R}^*) \mathbf{I} - \mathbf{R}^\top \mathbf{R}^*)$  satisfies  $\|\mathbf{E}(\mathbf{R}, \mathbf{R}^*)\|_F \leq \sqrt{3}$ . Also, by construction of the IDA-PBC

controller [15]:

$$\dot{\mathbf{p}}_e = -\mathbf{e} - \mathbf{K}_d \mathbf{M}^{-1} \mathbf{p}_e - \mathbf{W} \mathbf{e}_a \quad (18)$$

Consider the adaptation law  $\dot{\mathbf{a}} = c_1 \mathbf{W}^\top \mathbf{e} + c_2 \mathbf{W}^\top \mathbf{M}^{-1} \mathbf{p}_e$  in (14) with  $c_1 = c_p = c_R$  and  $c_2 = c_v = c_\omega$  and the Lyapunov function candidate:

$$\mathcal{V} = \mathcal{H}_d + \frac{c_1}{c_2} \frac{d}{dt} V_d + \frac{1}{2c_2} \|\mathbf{e}_a\|_2^2. \quad (19)$$

where  $V_d$  is the potential energy of the desired Hamiltonian in (10). The time derivative of  $V_d$  satisfies:

$$\frac{d}{dt} V_d = \mathbf{e}_v^\top \mathbf{e}_p + \mathbf{e}_\omega^\top \mathbf{e}_R = \mathbf{e}^\top \mathbf{M}^{-1} \mathbf{p}_e. \quad (20)$$

For  $\mathbf{z} := [\|\mathbf{e}\| \ \|\mathbf{p}_e\|]^\top \in \mathbb{R}^2$ , the Lyapunov function candidate in (19) is bounded as:

$$\frac{1}{2} \mathbf{z}^\top \mathbf{Q}_1 \mathbf{z} + \frac{1}{2c_2} \|\mathbf{e}_a\|_2^2 \leq \mathcal{V} \leq \frac{1}{2} \mathbf{z}^\top \mathbf{Q}_2 \mathbf{z} + \frac{1}{2c_2} \|\mathbf{e}_a\|_2^2, \quad (21)$$

where the matrices  $\mathbf{Q}_1$  and  $\mathbf{Q}_2$  are:

$$\begin{aligned} \mathbf{Q}_1 &= \begin{bmatrix} \min\{k_p, k_R\} & -\frac{c_1}{c_2} \lambda_{\max}(\mathbf{M}^{-1}) \\ -\frac{c_1}{c_2} \lambda_{\max}(\mathbf{M}^{-1}) & \lambda_{\min}(\mathbf{M}^{-1}) \end{bmatrix} \\ \mathbf{Q}_2 &= \begin{bmatrix} \max\{k_p, \frac{2k_R}{2-\alpha}\} & \frac{c_1}{c_2} \lambda_{\max}(\mathbf{M}^{-1}) \\ \frac{c_1}{c_2} \lambda_{\max}(\mathbf{M}^{-1}) & \lambda_{\max}(\mathbf{M}^{-1}) \end{bmatrix}. \end{aligned} \quad (22)$$

The time derivative of the Lyapunov candidate satisfies:

$$\begin{aligned} \frac{d}{dt} \mathcal{V} &= \mathbf{p}_e^\top \mathbf{M}^{-1} \dot{\mathbf{p}}_e + \mathbf{e}^\top \mathbf{M}^{-1} \dot{\mathbf{p}}_e \\ &\quad + \frac{c_1}{c_2} \mathbf{e}^\top \mathbf{M}^{-1} \dot{\mathbf{p}}_e + \frac{c_1}{c_2} \dot{\mathbf{e}}^\top \mathbf{M}^{-1} \mathbf{p}_e + \frac{1}{c_2} \mathbf{e}_a^\top \dot{\mathbf{a}} \\ &= -\mathbf{p}_e^\top \mathbf{M}^{-1} \mathbf{K}_d \mathbf{M}^{-1} \mathbf{p}_e \\ &\quad - \frac{c_1}{c_2} \mathbf{e}^\top \mathbf{M}^{-1} \mathbf{e} - \frac{c_1}{c_2} \mathbf{e}^\top \mathbf{M}^{-1} \mathbf{K}_d \mathbf{M}^{-1} \mathbf{p}_e \\ &\quad + \frac{c_1}{c_2} \mathbf{e}^\top \begin{bmatrix} \hat{\boldsymbol{\omega}} & \mathbf{0} \\ \mathbf{0} & \mathbf{0} \end{bmatrix} \mathbf{M}^{-1} \mathbf{p}_e \\ &\quad + \frac{c_1}{c_2} \mathbf{e}^\top \begin{bmatrix} \mathbf{R}^\top \mathbf{R}^* \hat{\boldsymbol{\omega}}^* \mathbf{R}^{*\top} \mathbf{R} & \mathbf{0} \\ \mathbf{0} & \mathbf{0} \end{bmatrix} \mathbf{M}^{-1} \mathbf{p}_e \\ &\quad + \frac{c_1}{c_2} \mathbf{p}_e^\top \mathbf{M}^{-1} \begin{bmatrix} k_p \mathbf{I} & \mathbf{0} \\ \mathbf{0} & k_R \mathbf{E}(\mathbf{R}, \mathbf{R}^*) \end{bmatrix} \mathbf{M}^{-1} \mathbf{p}_e, \end{aligned}$$

where we used (18), (17), and that  $\boldsymbol{\omega} = \mathbf{e}_\omega + \mathbf{R}^\top \mathbf{R}^* \boldsymbol{\omega}^*$  by definition of  $\mathbf{e}_\omega$ . Hence, on the domain  $\mathcal{T}$ , we have:

$$\frac{d}{dt} \mathcal{V} \leq -\mathbf{z}^\top \mathbf{Q}_3 \mathbf{z} = -\mathbf{z}^\top \begin{bmatrix} q_1 & q_2 \\ q_2 & q_3 \end{bmatrix} \mathbf{z}, \quad (23)$$

where the elements of  $\mathbf{Q}_3$  are:

$$\begin{aligned} q_1 &= \frac{c_1}{c_2} \lambda_{\min}(\mathbf{M}^{-1}), \\ q_2 &= -\frac{c_1}{c_2} (\lambda_{\max}(\mathbf{M}^{-1} \mathbf{K}_d \mathbf{M}^{-1}) + \beta + \gamma \lambda_{\max}(\mathbf{M}^{-1})), \\ q_3 &= \lambda_{\min}(\mathbf{M}^{-1} \mathbf{K}_d \mathbf{M}^{-1}) - \frac{c_1}{c_2} \max\{k_p, \sqrt{3}k_R\} \lambda_{\max}^2(\mathbf{M}^{-1}). \end{aligned}$$

Since  $k_p, k_R, \mathbf{K}_d = \text{diag}(k_v \mathbf{I}, k_\omega \mathbf{I})$  can be chosen arbitrarily large, there exists some choice of parameters that ensures that the matrices  $\mathbf{Q}_1, \mathbf{Q}_2$ , and  $\mathbf{Q}_3$  are positive definite. By the LaSalle-Yoshizawa theorem [17, Thm. A.8], the tracking errors  $\mathbf{e}, \mathbf{p}_e$  are asymptotically stable, while the estimation error  $\mathbf{e}_a$  is stable and uniformly bounded.  $\square$

## REFERENCES

- [1] L. Ljung, "System identification," *Wiley encyclopedia of electrical and electronics engineering*, 1999.
- [2] M. P. Deisenroth, D. Fox, and C. E. Rasmussen, "Gaussian processes for data-efficient learning in robotics and control," *IEEE Transactions on Pattern Analysis and Machine Intelligence*, vol. 37, no. 2, pp. 408–423, 2015.
- [3] F. Berkenkamp, A. P. Schoellig, and A. Krause, "Safe controller optimization for quadrotors with gaussian processes," in *IEEE International Conference on Robotics and Automation (ICRA)*, 2016, pp. 491–496.
- [4] A. H. Chang, C. M. Hubicki, J. J. Aguilar, D. I. Goldman, A. D. Ames, and P. A. Vela, "Learning to jump in granular media: Unifying optimal control synthesis with gaussian process-based regression," in *IEEE International Conference on Robotics and Automation (ICRA)*, 2017, pp. 2154–2160.
- [5] L. Hewing, J. Kabzan, and M. N. Zeilinger, "Cautious model predictive control using gaussian process regression," *IEEE Transactions on Control Systems Technology*, vol. 28, no. 6, 2019.
- [6] J. Kabzan, L. Hewing, A. Liniger, and M. N. Zeilinger, "Learning-based model predictive control for autonomous racing," *IEEE Robotics and Automation Letters*, vol. 4, no. 4, pp. 3363–3370, 2019.
- [7] G. Torrente, E. Kaufmann, P. Föhn, and D. Scaramuzza, "Data-driven mpc for quadrotors," *IEEE Robotics and Automation Letters*, vol. 6, no. 2, pp. 3769–3776, 2021.
- [8] M. Raissi, P. Perdikaris, and G. E. Karniadakis, "Multistep neural networks for data-driven discovery of nonlinear dynamical systems," *arXiv preprint arXiv:1801.01236*, 2018.
- [9] K. Chua, R. Calandra, R. McAllister, and S. Levine, "Deep reinforcement learning in a handful of trials using probabilistic dynamics models," in *Advances in Neural Information Processing Systems (NeurIPS)*, 2018.
- [10] D. Nguyen-Tuong and J. Peters, "Model learning for robot control: a survey," *Cognitive processing*, vol. 12, no. 4, 2011.
- [11] A. Sanchez-Gonzalez, N. Heess, J. T. Springenberg, J. Merel, M. Riedmiller, R. Hadsell, and P. Battaglia, "Graph networks as learnable physics engines for inference and control," in *International Conference on Machine Learning (ICML)*, 2018.
- [12] S. Greydanus, M. Dzamba, and J. Yosinski, "Hamiltonian neural networks," in *Advances in Neural Information Processing Systems (NeurIPS)*, vol. 32, 2019.
- [13] M. Lutter, K. Listmann, and J. Peters, "Deep Lagrangian Networks for end-to-end learning of energy-based control for under-actuated systems," in *IEEE/RSJ International Conference on Intelligent Robots and Systems (IROS)*, 2019.
- [14] Y. D. Zhong, B. Dey, and A. Chakraborty, "Symplectic ODE-Net: learning Hamiltonian dynamics with control," in *International Conference on Learning Representations (ICLR)*, 2019.
- [15] T. Duong and N. Atanasov, "Hamiltonian-based Neural ODE Networks on the SE(3) Manifold For Dynamics Learning and Control," in *Proceedings of Robotics: Science and Systems*, Virtual, July 2021.
- [16] K. S. Narendra and A. M. Annaswamy, *Stable adaptive systems*. Prentice Hall, 1989.
- [17] M. Krstic, P. V. Kokotovic, and I. Kanellakopoulos, *Nonlinear and adaptive control design*. John Wiley & Sons, Inc., 1995.
- [18] P. A. Ioannou and J. Sun, *Robust adaptive control*. Prentice Hall, 1996.
- [19] N. Hovakimyan and C. Cao,  *$\mathcal{L}_1$  adaptive control theory: Guaranteed robustness with fast adaptation*. SIAM, 2010.
- [20] R. M. Sanner and J.-J. E. Slotine, "Gaussian networks for direct adaptive control," in *1991 American control conference*. IEEE, 1991, pp. 2153–2159.
- [21] A. Gahlawat, P. Zhao, A. Patterson, N. Hovakimyan, and E. Theodorou, "L1-gp: L1 adaptive control with bayesian learning," in *Proceedings of the 2nd Conference on Learning for Dynamics and Control*, ser. Proceedings of Machine Learning Research, vol. 120. PMLR, 10–11 Jun 2020, pp. 826–837. [Online]. Available: <https://proceedings.mlr.press/v120/gahlawat20a.html>
- [22] R. C. Grande, G. Chowdhary, and J. P. How, "Nonparametric adaptive control using gaussian processes with online hyperparameter estimation," in *52nd IEEE Conference on Decision and Control*. IEEE, 2013, pp. 861–867.
- [23] G. Joshi and G. Chowdhary, "Deep model reference adaptive control," in *2019 IEEE 58th Conference on Decision and Control (CDC)*. IEEE, 2019, pp. 4601–4608.
- [24] G. Joshi, J. Virdi, and G. Chowdhary, "Asynchronous deep model reference adaptive control," *arXiv preprint arXiv:2011.02920*, 2020.
- [25] M. O'Connell, G. Shi, X. Shi, and S.-J. Chung, "Meta-learning-based robust adaptive flight control under uncertain wind conditions," *arXiv preprint arXiv:2103.01932*, 2021.
- [26] J. Harrison, A. Sharma, R. Calandra, and M. Pavone, "Control adaptation via meta-learning dynamics," in *Workshop on Meta-Learning at NeurIPS*, vol. 2018, 2018.
- [27] S. M. Richards, N. Azizan, J.-J. Slotine, and M. Pavone, "Adaptive-Control-Oriented Meta-Learning for Nonlinear Systems," in *Proceedings of Robotics: Science and Systems*, Virtual, July 2021.
- [28] J. Harrison, A. Sharma, and M. Pavone, "Meta-learning priors for efficient online bayesian regression," *arXiv preprint arXiv:1807.08912*, 2018.
- [29] G. Tao, "Multivariable adaptive control: A survey," *Automatica*, vol. 50, no. 11, pp. 2737–2764, 2014.
- [30] J.-J. E. Slotine and W. Li, "On the adaptive control of robot manipulators," *The International Journal of Robotics Research*, vol. 6, no. 3, pp. 49–59, 1987.
- [31] —, "Composite adaptive control of robot manipulators," *Automatica*, vol. 25, no. 4, pp. 509–519, 1989.
- [32] J.-J. E. Slotine and M. Di Benedetto, "Hamiltonian adaptive control of spacecraft," *IEEE Transactions on Automatic Control*, vol. 35, no. 7, pp. 848–852, 1990.
- [33] J.-J. E. Slotine and W. Li, *Applied nonlinear control*. Prentice Hall, 1991, vol. 199, no. 1.
- [34] D. A. Dirks and J. M. Scherpen, "Structure preserving adaptive control of port-hamiltonian systems," *IEEE Transactions on Automatic Control*, vol. 57, no. 11, pp. 2880–2885, 2012.
- [35] D. Dirks and J. M. Scherpen, "Adaptive control of port-hamiltonian systems," in *Proceedings of the 19th International Symposium on Mathematical Theory of Networks and Systems—MTNS*, vol. 5, no. 9, 2010.
- [36] S. S. Sastry and A. Isidori, "Adaptive control of linearizable systems," *IEEE Transactions on Automatic Control*, vol. 34, no. 11, pp. 1123–1131, 1989.
- [37] D. Hanover, P. Foehn, S. Sun, E. Kaufmann, and D. Scaramuzza, "Performance, Precision, and Payloads: Adaptive Nonlinear MPC for Quadrotors," in *arXiv cs.RO: 2109.04210*, 2021.
- [38] S. P. Nageshwar, G. A. Lopes, D. Jeltsema, and R. Babuška, "Port-hamiltonian systems in adaptive and learning control: A survey," *IEEE Transactions on Automatic Control*, vol. 61, no. 5, pp. 1223–1238, 2015.
- [39] V. Adetola, D. DeHaan, and M. Guay, "Adaptive model predictive control for constrained nonlinear systems," *Systems & Control Letters*, vol. 58, no. 5, pp. 320–326, 2009.
- [40] T. A. N. Heirung, B. E. Ydstie, and B. Foss, "Dual adaptive model predictive control," *Automatica*, vol. 80, pp. 340–348, 2017.
- [41] M. Lorenzen, F. Allgöwer, and M. Cannon, "Adaptive model predictive control with robust constraint satisfaction," *IFAC-PapersOnLine*, vol. 50, no. 1, pp. 3313–3318, 2017.
- [42] K. Pereida and A. P. Schoellig, "Adaptive model predictive control for high-accuracy trajectory tracking in changing conditions," in *2018 IEEE/RSJ International Conference on Intelligent Robots and Systems (IROS)*. IEEE, 2018, pp. 7831–7837.
- [43] T. Fernando, J. Chandiramani, T. Lee, and H. Gutierrez, "Robust adaptive geometric tracking controls on so(3) with an application to the attitude dynamics of a quadrotor uav," in *2011 50th IEEE conference on decision and control and European control conference*. IEEE, 2011, pp. 7380–7385.
- [44] T. Lee, "Robust adaptive attitude tracking on so(3) with an application to a quadrotor uav," *IEEE Transactions on Control Systems Technology*, vol. 21, no. 5, pp. 1924–1930, 2012.
- [45] F. A. Goodarzi, D. Lee, and T. Lee, "Geometric adaptive tracking control of a quadrotor unmanned aerial vehicle on se(3) for agile maneuvers," *Journal of Dynamic Systems, Measurement, and Control*, vol. 137, no. 9, p. 091007, 2015.
- [46] M. Bisheban and T. Lee, "Geometric adaptive control for a quadrotor uav with wind disturbance rejection," in *2018 IEEE Conference on Decision and Control (CDC)*. IEEE, 2018, pp. 2816–2821.
- [47] —, "Geometric adaptive control with neural networks for a quadrotor in wind fields," *IEEE Transactions on Control Systems Technology*, vol. 29, no. 4, pp. 1533–1548, 2020.

- [48] G. Shi, K. Azizzadenesheli, S.-J. Chung, and Y. Yue, "Meta-adaptive nonlinear control: Theory and algorithms," *arXiv preprint arXiv:2106.06098*, 2021.
- [49] T. Lee, M. Leok, and N. H. McClamroch, *Global formulations of Lagrangian and Hamiltonian dynamics on manifolds*. Springer, 2017.
- [50] R. T. Chen, Y. Rubanova, J. Bettencourt, and D. Duvenaud, "Neural ordinary differential equations," in *Advances in Neural Information Processing Systems (NeurIPS)*, 2018.
- [51] J. Delmerico and D. Scaramuzza, "A benchmark comparison of monocular visual-inertial odometry algorithms for flying robots," in *IEEE International Conference on Robotics and Automation (ICRA)*, 2018.
- [52] S. A. S. Mohamed, M. Haghbayan, T. Westerlund, J. Heikkonen, H. Tenhunen, and J. Plosila, "A survey on odometry for autonomous navigation systems," *IEEE Access*, vol. 7, 2019.
- [53] A. Van Der Schaft and D. Jeltsema, "Port-Hamiltonian systems theory: An introductory overview," *Foundations and Trends in Systems and Control*, vol. 1, no. 2-3, 2014.
- [54] J. Panerati, H. Zheng, S. Zhou, J. Xu, A. Prorok, and A. P. Schöellig, "Learning to fly: a pybullet gym environment to learn the control of multiple nano-quadcopters," <https://github.com/utiasDSL/gym-pybullet-drones>, 2020.
- [55] T. Lee, M. Leok, and N. H. McClamroch, "Geometric tracking control of a quadrotor UAV on  $SE(3)$ ," in *IEEE Conference on Decision and Control (CDC)*, 2010.
- [56] T. Lee, "Robust Adaptive Attitude Tracking on  $SO(3)$  with an Application to a Quadrotor UAV," *IEEE Transactions on Control Systems Technology*, vol. 21, no. 5, pp. 1924–1930, 2013.